

# Self-assembly Syntheses, Crystal Structures and Quantum Chemistry of Two $\text{UO}_2^{2+}$ Complexes<sup>①</sup>

TAN Yu-Xing<sup>a②</sup> NAN Xiao-Long<sup>b</sup> TAN Yan-Liang<sup>c</sup>  
ZHANG Zhi-Jian<sup>a</sup> JIANG Wu-Jiu<sup>a</sup>

<sup>a</sup> (Key Laboratory of Functional Metal-organic Compounds of Hunan Province, Key Laboratory of Functional Organometallic Materials, University of Hunan Province, Hunan Provincial Engineering Research Center for Monitoring and Treatment of Heavy Metals Pollution in the Upper Reaches of Xiangjiang River, College of Chemistry and Materials Science, Hengyang Normal University, Hengyang, Hunan 421008, China)

<sup>b</sup> (Nuclear Bureau of Hunan Province Nuclear Industry Brigade 306, Hengyang, Hunan 421008, China)

<sup>c</sup> (Hunan Provincial Engineering Research Center for Uranium Mineral Exploration Technology, College of Physics and Electronic Engineering, Hengyang Normal University, Hengyang, Hunan 421002, China)

**ABSTRACT** Two  $\text{UO}_2^{2+}$  complexes  $\{[\text{C}_5\text{H}_4\text{N}(\text{O})\text{C}=\text{N}-\text{N}=\text{C}(\text{Ph})-(\text{Ph})\text{C}=\text{N}-\text{N}=\text{C}(\text{O})-\text{C}_5\text{H}_4\text{N}]_2\text{UO}_2(\text{CH}_3\text{OH})\}$  (**I**) and  $\{[\text{C}_5\text{H}_4\text{N}(\text{O})\text{C}=\text{N}-\text{N}=\text{C}(\text{Ph})-(\text{Ph})\text{C}=\text{N}-\text{N}=\text{C}(\text{O})-\text{C}_5\text{H}_4\text{N}]_2\text{UO}_2(\text{C}_5\text{H}_4\text{N}(\text{O})\text{C}=\text{N}-\text{NH}_2)\}$  (**II**) were synthesized and characterized by IR, elemental analysis and thermal stability analysis, and the crystal structures were determined by X-ray diffraction. The crystal of complex **I** belongs to monoclinic system, space group  $P2_1/n$  with  $a = 11.7678(4)$ ,  $b = 16.9667(6)$ ,  $c = 14.3051(5)$  Å,  $\beta = 98.918(3)^\circ$ ,  $Z = 4$ ,  $V = 2821.64(17)$  Å<sup>3</sup>,  $D_c = 1.837$  Mg m<sup>-3</sup>,  $\mu(\text{MoK}\alpha) = 5.805$  mm<sup>-1</sup>,  $F(000) = 1504$ ,  $R = 0.0346$  and  $wR = 0.0688$ . The crystal of complex **II** is of triclinic system, space group  $P\bar{1}$  with  $a = 11.6417(5)$ ,  $b = 11.7297(5)$ ,  $c = 14.2197(5)$  Å,  $\alpha = 71.697(4)^\circ$ ,  $\beta = 86.020(3)^\circ$ ,  $\gamma = 71.572(4)^\circ$ ,  $Z = 2$ ,  $V = 1748.02(12)$  Å<sup>3</sup>,  $D_c = 1.742$  Mg m<sup>-3</sup>,  $\mu(\text{MoK}\alpha) = 4.704$  mm<sup>-1</sup>,  $F(000) = 894$ ,  $R = 0.0283$  and  $wR = 0.0537$ . The U1 is a seven-coordinate pentagonal bipyramidal configuration in **I** and an eight-coordinate hexagonal dipyramidal configuration in **II**. The thermal stability and quantum chemical calculations of **I** and **II** were also investigated.

**Keywords:**  $\text{UO}_2^{2+}$  complexes, synthesis, crystal structure, quantum chemistry;

**DOI:** 10.14102/j.cnki.0254-5861.2011-3223

## 1 INTRODUCTION

Uranium is a radioactive metal element, which is the most important nuclear fuel in nature, and an element that has attracted much attention in the development of nuclear energy<sup>[1-3]</sup>. At the beginning of the nuclear fuel cycle, the release of uranium was inevitable during the mining and purification of uranium; at the end of the nuclear fuel cycle, radioactive waste will also contain a large amount of unreacted uranium<sup>[4, 5]</sup>. At present, many countries in the world are stepping up research on the disposal of nuclear waste to use chemical methods for the treatment and reuse of nuclear waste. Therefore, studying the coordination chemistry of uranium, understanding the bonding characteristics of

uranium, and discussing the structures and properties of novel uranyl complexes can solve the safe storage problems of nuclear waste and radioactive pollution. And it can provide experimental accumulation and new ideas.

The electron shell of uranium is  $[\text{Rn}]5f^36d^17s^2$ , and the neutrons of  $5f$  orbital have a shielding effect on the outer electrons, which makes uranium have a changeable oxidation state. Among them, the +6 valence is the most stable, the center ionic electrical properties of the high oxidation state are high, the ionic radius is large, and the attraction of the ligand is strong, and more ligands can be attracted to form a highly complement number of mating units<sup>[6-9]</sup>. Therefore, two unreported uranyl complexes have been designed to synthesize the multidentate organic ligand containing ONO and

Received 19 April 2021; accepted 24 June 2021 (CCDC 2077408 and 2077409)

① Supported by the Foundation of Hunan Provincial Engineering Research Center for Uranium Exploration Technology (No. YK20K03)

② Corresponding author. E-mail: tanyuxing@hynu.edu.cn

uranyl acetate by self-assembly reaction in this paper, and the studies on two complexes have been performed with quantum chemistry calculation. The stabilities, some frontier molecular orbital energies and composition characteristics of some frontier molecular orbitals of the compound have been investigated. It provides a certain theoretical significance for the research of nuclear waste treatment, catalysis, mineralogues and energy.

## 2 EXPERIMENTAL

### 2.1 Instruments and reagents

Infrared spectrum (KBr) was recorded by the Prestige-21 infrared spectrometer (Japan Shimadzu,  $4000\sim 400\text{ cm}^{-1}$ ). The elemental analysis was determined by PE-2400(II) elemental analyzer. Crystallographic data of the complexes were collected on a Bruker SMART APEX II CCD diffractometer. Melting points were determined using an X4 digital microscopic melting point apparatus without correction (Beijing Tektronix Instrument Co. Ltd.). Thermogravimetric analyses (TGA) were recorded on a NETZSCH TG 209 F3 instrument at a heating rate of  $20\text{ }^\circ\text{C}\cdot\text{min}^{-1}$  from  $40$  to  $800\text{ }^\circ\text{C}$  under air. Powder X-ray diffraction (PXRD) pattern of the complex was collected on a Shimadzu X-ray diffractometer

XRD6100 with the  $\text{CuK}\alpha$  radiation ( $\lambda = 1.5406\text{ \AA}$ ) at room temperature and  $2\theta$  ranging from  $5^\circ$  to  $50^\circ$ .

The reagents used in the experiment were all analytical reagents, and used directly without further purification.

### 2.2 Synthesis of the complexes

A mixture of 4-pyridoylhydrazine (2.0 mmol), benzil (1.0 mmol), uranyl acetate (1 mmol) and  $\text{CH}_3\text{OH}$  (10.0 mL) was added in a Teflon-lined stainless-vessel (20.0 mL), and heated at  $120\text{ }^\circ\text{C}$  for 10.0 h, then cooled to room temperature at a rate of  $5\text{ }^\circ\text{C}\cdot\text{h}^{-1}$ . The crystals of **I** were collected. Complex **I** was a red block crystal. Yield: 63%. m.p.:  $116\sim 118\text{ }^\circ\text{C}$  (dec.). Anal. Calcd. ( $\text{C}_{28}\text{H}_{26}\text{N}_6\text{O}_6\text{U}$ ): C, 43.08; H, 3.36; N 10.77%. Found: C, 43.14; H, 3.41; N, 10.69%. FT-IR (KBr,  $\text{cm}^{-1}$ ): 3090, 3065, 3034, 2931, 2819, 1607, 1570, 1528, 1501, 1472, 1373, 1296, 1155, 1061, 926, 878, 843, 783, 754, 696, 687, 615, 538.

Complex **II** was prepared in a similar procedure (Fig. 1) as **I** by 4-pyridoylhydrazine (2.0 mmol) in place of 3-pyridoylhydrazine (2.0 mmol). The product was a bronze block crystal with the yield of 61% (based on 3-pyridoylhydrazine). m.p.:  $105\sim 107\text{ }^\circ\text{C}$  (dec.). Anal. Calcd. ( $\text{C}_{34}\text{H}_{32}\text{N}_9\text{O}_7\text{U}$ ): C, 44.55; H, 3.52; N, 13.75%. Found: C, 44.54; H, 3.58; N, 13.82%. FT-IR (KBr,  $\text{cm}^{-1}$ ): 3291, 3198, 3173, 3057, 1657, 1593, 1541, 1504, 1485, 1474, 1406, 1381, 1335, 1319, 1211, 1165, 1111, 1059, 1026, 907, 881, 827, 731, 698, 538, 459.

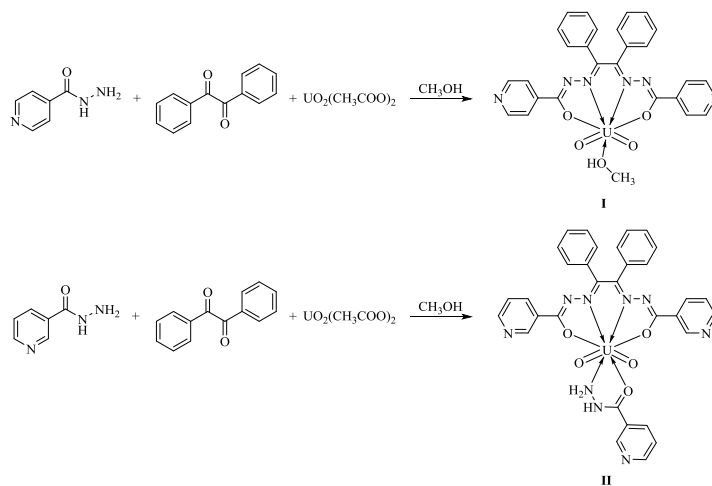


Fig. 1. Syntheses of the complexes

### 2.3 Crystal structure determination

Suitable single crystals with dimensions of  $0.13\text{mm} \times 0.11\text{mm} \times 0.10\text{mm}$  (**I**) and  $0.13\text{mm} \times 0.12\text{mm} \times 0.09\text{mm}$  (**II**) were selected for data collection at 100 K on a Bruker SMART APEX II CCD diffractometer equipped with graphite-monochromated  $\text{MoK}\alpha$  radiation ( $\lambda = 0.71073\text{ \AA}$ ) using a  $\varphi\text{-}\omega$  mode. All the data were corrected by  $L_p$  factors and empirical absorbance. The structures were solved by

direct methods. All non-hydrogen atoms were determined in successive difference Fourier synthesis, and hydrogen atoms were added according to theoretical models or located from the Fourier maps. All hydrogen and non-hydrogen atoms were refined by their isotropic and anisotropic thermal parameters through full-matrix least-squares techniques. All calculations were completed by the SHELXTL-97<sup>[10]</sup> program. For complex **I**, a total of 13993 reflections were obtained in the

range of  $2.09 < \theta < 26.00^\circ$  with 5557 unique ones ( $R_{\text{int}} = 0.0405$ ),  $S = 1.030$ ,  $(\Delta\rho)_{\text{max}} = 1.631$  and  $(\Delta\rho)_{\text{min}} = -1.484 \text{ e}/\text{\AA}^3$ , max transmission was 1.00000, min transmission was 0.68535, and the completeness was 100.0%. For complex **II**, a total of 14220 reflections were obtained in the range of

$1.92 < \theta < 26.00^\circ$  with 6876 unique ones ( $R_{\text{int}} = 0.0346$ ),  $S = 1.023$ ,  $(\Delta\rho)_{\text{max}} = 1.114$ ,  $(\Delta\rho)_{\text{min}} = -1.017 \text{ e}/\text{\AA}^3$ , max transmission was 1.00000, min transmission was 0.72112, and the completeness was 100.0%. The selected bond lengths and bond angles for **I** and **II** are listed in Table 1.

Table 1. Selected Bond Lengths (Å) and Bond Angles ( $^\circ$ ) for **I** and **II**

I					
Bond	Dist.	Bond	Dist.	Bond	Dist.
U(1)–O(6)	1.776(3)	U(1)–O(5)	1.777(3)	U(1)–O(1)	2.325(3)
U(1)–O(2)	2.340(3)	U(1)–O(3)	2.378(4)	U(1)–N(4)	2.514(4)
U(1)–N(3)	2.529(4)				
Angle	( $^\circ$ )	Angle	( $^\circ$ )	Angle	( $^\circ$ )
O(6)–U(1)–O(5)	177.95(15)	O(6)–U(1)–O(1)	89.31(13)	O(5)–U(1)–O(1)	90.96(13)
O(6)–U(1)–O(2)	91.30(13)	O(5)–U(1)–O(2)	88.76(13)	O(1)–U(1)–O(2)	171.09(11)
O(6)–U(1)–O(3)	88.32(14)	O(5)–U(1)–O(3)	93.73(14)	O(1)–U(1)–O(3)	86.85(11)
O(2)–U(1)–O(3)	84.28(11)	O(6)–U(1)–N(4)	89.27(14)	O(5)–U(1)–N(4)	88.91(14)
O(1)–U(1)–N(4)	124.93(12)	O(2)–U(1)–N(4)	63.98(11)	O(3)–U(1)–N(4)	148.10(12)
O(6)–U(1)–N(3)	84.79(14)	O(5)–U(1)–N(3)	93.50(14)	O(1)–U(1)–N(3)	63.70(11)
O(2)–U(1)–N(3)	125.21(11)	O(3)–U(1)–N(3)	149.75(12)	N(4)–U(1)–N(3)	61.35(11)
II					
Bond	Dist.	Bond	Dist.	Bond	Dist.
U(1)–O(4)	1.779(3)	U(1)–O(3)	1.783(3)	U(1)–O(1)	2.355(3)
U(1)–O(2)	2.396(2)	U(1)–O(5)	2.524(2)	U(1)–N(5)	2.584(3)
U(1)–N(6)	2.600(3)	U(1)–N(8)	2.639(3)		
Angle	( $^\circ$ )	Angle	( $^\circ$ )	Angle	( $^\circ$ )
O(4)–U(1)–O(3)	177.42(9)	O(4)–U(1)–O(1)	87.45(11)	O(3)–U(1)–O(1)	93.19(11)
O(4)–U(1)–O(2)	89.53(10)	O(3)–U(1)–O(2)	89.91(10)	O(1)–U(1)–O(2)	176.35(9)
O(4)–U(1)–O(5)	98.70(9)	O(3)–U(1)–O(5)	83.79(9)	O(1)–U(1)–O(5)	61.64(8)
O(2)–U(1)–O(5)	116.89(8)	O(4)–U(1)–N(5)	90.13(10)	O(3)–U(1)–N(5)	87.99(10)
O(1)–U(1)–N(5)	61.42(8)	O(2)–U(1)–N(5)	120.67(8)	O(5)–U(1)–N(5)	121.75(8)
O(4)–U(1)–N(6)	89.63(10)	O(3)–U(1)–N(6)	87.90(10)	O(1)–U(1)–N(6)	121.38(8)
O(2)–U(1)–N(6)	60.62(8)	O(5)–U(1)–N(6)	171.37(9)	N(5)–U(1)–N(6)	60.05(9)
O(4)–U(1)–N(8)	85.99(10)	O(3)–U(1)–N(8)	95.86(10)	O(1)–U(1)–N(8)	119.12(8)
O(2)–U(1)–N(8)	58.56(8)	O(5)–U(1)–N(8)	59.82(8)	N(5)–U(1)–N(8)	176.04(9)
N(6)–U(1)–N(8)	119.03(9)				

### 3 RESULTS AND DISCUSSION

#### 3.1 Synthesis

The solvothermal synthesis method was used to prepare complexes in this paper. Under a certain temperature, self-assembly of the reactants can form the final product, and the solvent heat method has an advantage over the ordinary synthetic method<sup>[11–13]</sup>. For example, (1) Under high temperature, the solvent gasification in the reactor has generated pressure such that some ligands dissolving in difficulty at room temperature can be dissolved, and the high temperature condition causes the solvent viscosity to decrease, thus facilitating the transfer between the substances; (2) The solvent reaction conditions are simple, fast and efficient and

easy to control with better reproducibility; (3) Under this condition, a novel compound that has an unexpected structure can be obtained by the self-assembly of the organic ligand.

Compared to the reactant ratio and conditions of the two reactions, only the position of the nitrogen atom on the pyridine ring was different, and the other is the same. However, two complexes are obtained by self-assembly reactions. It can be seen that the self-assembly reaction of the organic ligand does get a lot of novel compound molecules.

#### 3.2 Spectral analyses

In the infrared spectra of complexes **I** and **II**, the strong peaks at 925 and 906  $\text{cm}^{-1}$  and the weak ones at 842 and 827  $\text{cm}^{-1}$  are attributed to the symmetric and asymmetric stretching vibration peaks of  $\text{UO}_2^{2+}$ <sup>[14, 15]</sup>. It is a characteristic

peak of  $\text{UO}_2^{2+}$  complex, which is consistent with the position of the absorption peak reported in literature. The absorption peaks at 3090, 3065, 3034  $\text{cm}^{-1}$  in complex **I** and 3198, 3173, 3057  $\text{cm}^{-1}$  in **II** are assigned to the C–H stretching vibration absorption peaks on the aromatic ring of the complex. The absorption peaks at 2931, 2819  $\text{cm}^{-1}$  in **I** are due to the saturated C–H stretching vibration absorption peak, while the absence of a peak in **II** indicates no saturated C–H bond in this complex. This conclusion is consistent with the X-ray single-crystal diffraction results.

### 3.3 Structure description

The molecular structures of complexes **I** and **II** are shown in Fig. 2. Both of them contain a mononuclear  $\text{UO}_2^{2+}$  complex molecule, but the coordination modes of Th (IV) are different.

In complex **I**, the U1 adopts a seven-coordinate pentagonal

bipyramidal configuration.  $\text{UO}_2^{2+}$  forms a pentagonal bipyramidal configuration with the two nitrogen atoms (N(3), N(4)) and two oxygen atoms (O(1), O(2)) from the diacylhydrazone ligand and the one oxygen atom O(3) from the methanol. These five atoms form the equatorial plane of the pentagonal bipyramid, the axis of which is occupied by the two oxygen atoms on  $\text{UO}_2^{2+}$ . The bonds between oxygen or nitrogen atoms on the equatorial plane and U are similar to the reports<sup>[16, 17]</sup>.  $d_{\text{U1-O1}} = 2.325(3)$ ,  $d_{\text{U1-O2}} = 2.340(3)$ ,  $d_{\text{U1-O3}} = 2.378(4)$ ,  $d_{\text{U1-N3}} = 2.529(4)$  and  $d_{\text{U1-N4}} = 2.514(4)$  Å. The two O atoms are bonded from axial and uranium, with the U=O bonds to be 1.777(3) and 1.776(3) Å, respectively, and the O=U=O angle of 177.95(15) °, so it can be approximately considered to be on a straight line.

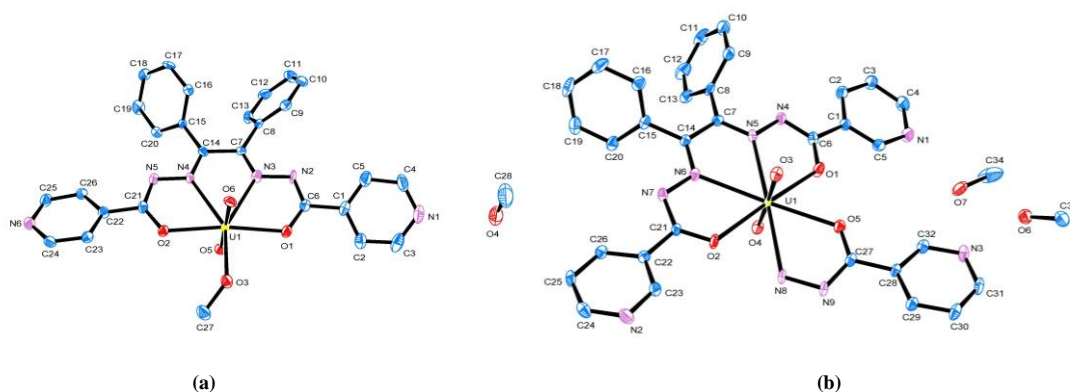


Fig. 2. Molecular structures of **I** (a) and **II** (b)

In complex **II**, the U1 is an eight-coordinate hexagonal bipyramidal configuration. The structures of complexes **II** and **I** are slightly different. Comparing complex **I** to **II**, another 3-pyridoylhydrazone molecule was involved in coordination by bidentate. Thereby, the U1 is eight-coordinated in complex **II**. Other parameters are similar to the literature<sup>[18, 19]</sup>.

### 3.4 XRD and TGA

To verify the purity of complexes, XRD of complexes **I** and **II** was performed<sup>[20, 21]</sup>. As shown in Fig. 3, the relevant positions of diffraction peaks in experimental patterns match well with those in the simulated ones, indicating good purity for complexes **I** and **II**.

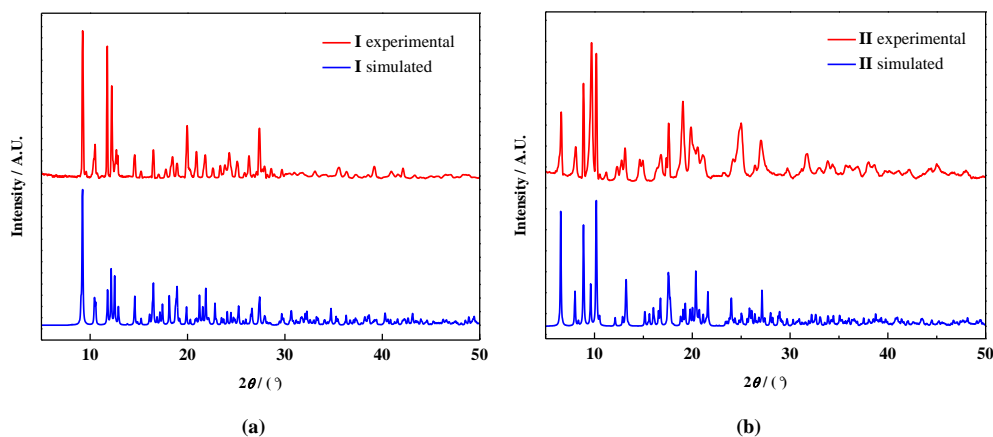


Fig. 3. XRD of complexes **I** (a) and **II** (b)

Thermal stabilities of both complexes are carried out using a NETZSCH TG 209 F3 thermogravimetric analyzer from 40 to 800 °C at a rate of 20 °C min<sup>-1</sup> under an air atmosphere at a flowing rate of 20.0 mL min<sup>-1</sup>. As shown in Fig. 4, with the increase of temperature, complexes **I** and **II** have a similar weight loss process. In the first stages, complexes **I** and **II** display a small weight loss at around 110 °C, corresponding to the departure of methanol molecule. The results were

consistent with X-ray single-crystal diffraction data. It shows that the molecule of the complex contains methanol. In the next stages, both complexes suffer complete decomposition until about 600 °C, corresponding to the removal of ligand. The remaining weight (35.6% (**I**) and 30.8% (**II**)) indicates the final products are UO<sub>2</sub> (34.5% (**I**) and 29.4% (**II**)). In summary, **I** and **II** are stable up to 100 °C.

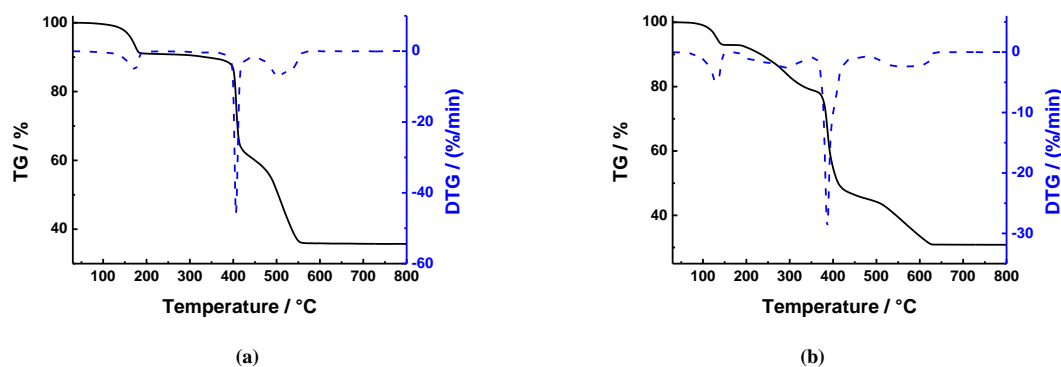


Fig. 4. TG-DTG curves for **I** (a) and **II** (b)

### 3.5 Quantum chemical

According to the atomic coordinates of the crystal structure, the total energy of the molecule and the energy of the frontier molecular orbital were calculated by the Gaussian 09W program at the B3lyp/mwb basis group level.

Complex **I**:  $E_T = -782.639337051$  a.u.,  $E_{HOMO} = -0.22101$  a.u.,  $E_{LUMO} = -0.10866$  a.u. and  $\Delta E_{LUMO-HOMO} = 0.11235$  a.u.. Complex **II**:  $E_T = -841.810598184$  a.u.,  $E_{HOMO} = -0.1944$  a.u.,  $E_{LUMO} = -0.1106$  a.u. and  $\Delta E_{LUMO-HOMO} = 0.0838$  a.u. It can be seen that the total energy and occupied orbital energy of the two complexes are both low, and the energy gap between the highest occupied and lowest unoccupied orbitals is small.

It shows that complexes **I** and **II** are more difficult to lose electrons and be oxidized.

In order to explore the electronic structure and bonding characteristics of both complexes, the molecular orbitals of **I** and **II** were analyzed. The squares sum of various atomic orbital coefficients participating in combination is used to express the contribution of this part in the molecular orbital, which is normalized. The atoms of compounds were divided into five parts. For **I** or **II**: (a) U atom; (b) O atom; (c) N atom; (d) C atom; (e) H atom. Five frontier occupied and unoccupied orbitals are taken respectively, and the calculated results are shown in Tables 2 and 3 as well as Figs. 5 and 6.

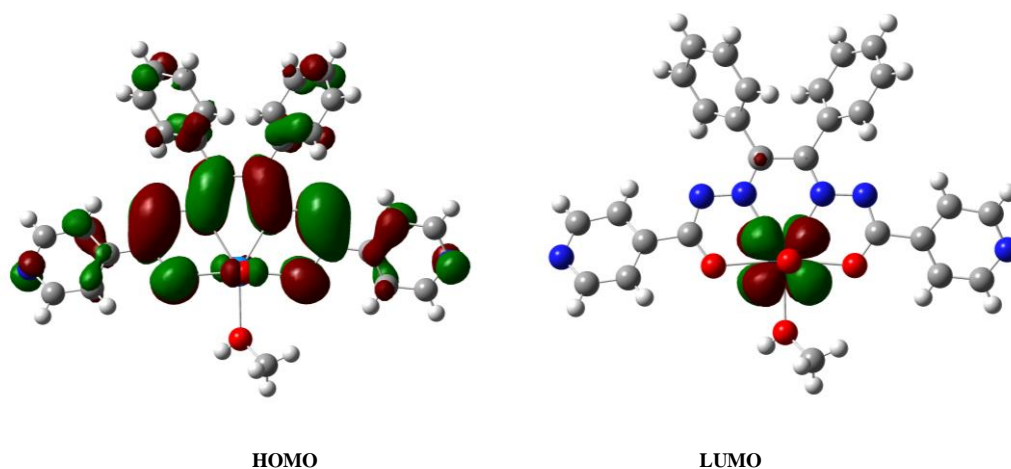


Fig. 5. Schematic diagram of the frontier MO for **I**

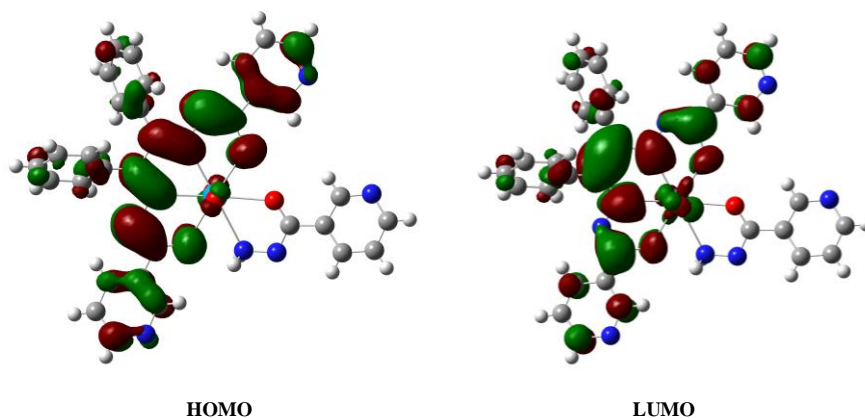


Fig. 6. Schematic diagram of the frontier MO for II

Table 2. Some Calculated Frontier Molecular Orbitals Composition of Complex I (%)

MO	$\epsilon/\text{Hartree}$	U	O	N	C	H
107	-0.2522	5.25084	5.45281	26.04255	62.84571	0.37827
108	-0.24636	1.13022	0.81525	51.44808	37.64035	8.94427
109	-0.24406	1.17399	1.33641	48.71464	40.59434	7.1563
110	-0.24202	1.83619	6.5815	30.62967	57.73136	2.84501
111 HOMO	-0.22101	0.98112	18.87537	44.92791	34.9036	0.31077
112 LUMO	-0.10866	97.03186	0.32815	0.42237	2.03976	0.16063
113	-0.10728	80.79693	0.52993	5.70415	12.75073	0.20825
114	-0.10389	93.92963	1.88016	1.33811	2.765	0.07869
115	-0.1007	19.81072	7.17446	24.90143	47.89401	0.21171
116	-0.09601	86.9384	4.59619	2.34665	5.73781	0.37357

Table 3. Some Calculated Frontier Molecular Orbitals Composition of Complex II (%)

MO	$\epsilon/\text{Hartree}$	U	O	N	C	H
126	-0.24961	7.50554	3.35016	45.28693	38.1423	5.71288
127	-0.24865	3.36804	9.4762	41.83891	41.69315	3.62018
128	-0.24614	5.15732	2.48214	50.06101	35.14033	7.1505
129	-0.21601	10.23696	18.34583	47.18023	23.19842	1.02464
130 HOMO	-0.1944	3.81108	21.4714	49.5335	24.1124	1.06082
131 LUMO	-0.1106	16.8301	5.07102	24.0405	53.7605	0.29027
132	-0.10562	97.15283	0.4477	0.60681	1.74595	0.01938
133	-0.1033	96.85568	1.26164	0.62252	1.18422	0.05925
134	-0.10306	67.65543	4.86094	10.91831	16.33138	0.21975
135	-0.08577	80.78102	3.96382	5.37255	9.78276	0.09298

By comparing the components of atomic orbitals of HOMO and LUMO in **I**, it can be seen that when excited from HOMO to LUMO orbitals, the electrons are mainly transferred from ligands to U atoms, so that the contributions of U atom are 97.03186%. When electrons are excited from HOMO to LUMO orbitals in **II**, they mainly transfer between the ligands, and some are transferred from the ligand to the U atom.

#### 4 CONCLUSION

Two  $\text{UO}_2^{2+}$  complexes have been synthesized and characterized. In complex **I**, the U1 is a seven-coordinate pentagonal bipyramidal configuration. In **II**, the U1 is an eight-coordinate hexagonal bipyramidal configuration. **I** and **II** are stable up to 100 °C. The quantum chemical has indicated that complexes **I** and **II** are more difficult to lose electrons and be oxidized.

## REFERENCES

- (1) Settle, F. A. Uranium to electricity: the chemistry of the nuclear fuel cycle. *J. Chem. Edu.* **2009**, 86, 316–323.
- (2) Gates, S. D.; Cassata, W. S. Application of the uranium-helium chronometer to the analysis of nuclear forensic materials. *Anal. Chem.* **2016**, 88, 12310–12315.
- (3) Alley, W. M.; Alley, R. The growing problem of stranded used nuclear fuel. *Environ. Sci. Technol.* **2014**, 48, 2091–2096.
- (4) Pastoor, K. J.; Kemp, R. S.; Jensen, M. P.; Shafer, J. C. Progress in uranium chemistry: driving advances in front-end nuclear fuel cycle forensics. *Inorg. Chem.* **2021**, DOI: 10.1021/acs.inorgchem.0c03390
- (5) Todd, T. A. Separations research for advanced nuclear fuel cycles. Nuclear energy and the environment. *American Chemical Society* **2010**, 13–18.
- (6) McSkimming, A.; Su, J.; Cheisson, T.; Gau, M. R.; Carroll, P. J.; Batista, E. R.; Yang, P.; Schelter, E. J. Coordination chemistry of a strongly-donating hydroxylamine with early actinides: an investigation of redox properties and electronic structure. *Inorg. Chem.* **2018**, 57, 4387–4394.
- (7) Yao, J.; Zheng, X. J.; Pan, Q. J.; Schreckenbach, G. Highly valence-diversified binuclear uranium complexes of a Schiff-base polypyrrrolic macrocycle: prediction of unusual structures, electronic properties, and formation reactions. *Inorg. Chem.* **2015**, 54, 5438–5449.
- (8) Marchenko, A.; Truflandier, L. A.; Autschbach, J. Uranyl carbonate complexes in aqueous solution and their ligand NMR chemical shifts and 17O quadrupolar relaxation studied by *ab initio* molecular dynamics. *Inorg. Chem.* **2017**, 56, 7384–7396.
- (9) Drouza, C.; Gramlich, V.; Sigalas, M. P.; Pashalidis, I.; Keramidis, A. D. Synthesis, structure, and solution dynamics of  $\text{UO}_2^{2+}$ -hydroxy ketone compounds  $[\text{UO}_2(\text{ma})_2(\text{H}_2\text{O})]$  and  $[\text{UO}_2(\text{dpp})(\text{Hdpp})_2(\text{H}_2\text{O})]\text{ClO}_4$  (ma = 3-Hydroxy-2-methyl-4-pyrone, Hdpp = 3-hydroxy-1,2-dimethyl-4(1H)-pyridone). *Inorg. Chem.* **2004**, 43, 8336–8345.
- (10) Sheldrick, G. M. *SHELXL-97, A Program for Crystal Structure Refinement*. Germany Geöttingen: University of Geöttingen **1997**.
- (11) Yang, J.; Quan, Z.; Kong, D.; Liu, X.; Lin, J.  $\text{Y}_2\text{O}_3: \text{Eu}^{3+}$  microspheres: solvothermal synthesis and luminescence properties. *Cryst. Growth Des.* **2007**, 7, 730–735.
- (12) Choi, J.; Gillan, E. G. Solvothermal synthesis of nanocrystalline copper nitride from an energetically unstable copper azide precursor. *Inorg. Chem.* **2005**, 44, 7385–7393.
- (13) Huang, W.; Jiang, Y.; Li, X.; Li, X.; Wang, J.; Wu, Q.; Liu, X. Solvothermal synthesis of microporous, crystalline covalent organic framework nanofibers and their colorimetric nanohybrid structures. *ACS Appl. Mater. Inter.* **2013**, 5, 8845–8849.
- (14) Wang, C. Synthesis, structural analysis and adsorption properties of the uranyl complex. *Chem. Reagent.* **2019**, 41, 431–436.
- (15) Ge, R.; Wu, S.; Zeng, L. W.; Li, F. Z.; Mei, L.; Liu, C. L. Synthesis, structure and physico-chemical properties of two uranyl complexes of cucurbiturils mediated by sulfate ions. *Sci. Sin. Chim.* **2019**, 49, 1073–1082.
- (16) Mackinnon, P. I.; Taylor, J. C. The crystal and molecular structure of dioxo bis(2,2,6,6-tetramethylheptane-3,5-dionato)methanol uranium (VI). *Polyhedron* **1983**, 2, 217–224.
- (17) Day, V. W.; Marks, T. J.; Wachter, W. A. Large metal ion-centered template reactions. Uranyl complex of cyclopentakis(2-iminoisindoline). *J. Am. Chem. Soc.* **1975**, 97, 4519–4527.
- (18) de Almeida, K. C. S.; Martins, T. S.; Isolani, P. C.; Vicentini, G.; Zukerman-Schpector, J. Uranyl nitrate complexes with diphenylsulfoxide and dibenzylsulfoxide: characterization, luminescence and structures. *J. Solid State Chem.* **2003**, 171, 230–234.
- (19) Gatto, C. C.; Schulz Lang, E.; Kupfer, A.; Hagenbach, A.; Wille, D.; Abram, U. Dioxouranium complexes with acetylpyridine benzoylhydrazones and related ligands. *Z. Anorg. Allg. Chem.* **2004**, 630, 735–741.
- (20) Jiang, W.; Yang, J.; Yan, G.; Zhou, S.; Liu, B.; Qiao, Y.; Zhou, T.; Wang, J.; Che, G. A novel 3-fold interpenetrated dia metal-organic framework as a heterogeneous catalyst for  $\text{CO}_2$  cycloaddition. *Inorg. Chem. Commun.* **2020**, 113, 107770.
- (21) Ren, S.; Jiang, W.; Wang, Q.; Li, Z.; Qiao, Y.; Che, G. Synthesis, structures and properties of six lanthanide complexes based on a 2-(2-carboxyphenyl)imidazo(4,5-f)-(1,10)phenanthroline ligand. *RSC Adv.* **2019**, 9, 3102–3112.